

# INVARIANT CROSS SECTIONS FOR $p + d \rightarrow {}^3A + \pi$ REACTIONS IN $\Delta$ -RESONANCE REGION

<sup>a</sup>S. Abdel-Samad, <sup>a</sup>J. Bojowald, <sup>d</sup>A. Budzanovski, <sup>i</sup>A. Chatterjee, <sup>g</sup>J. Ernst, <sup>h</sup>D. Frekers, <sup>a,c</sup>P. Hawranek, <sup>a,e</sup>J. Ilieva, <sup>c</sup>L. Jarczyk, <sup>a</sup>K. Kilian, <sup>d</sup>S. Kliczewski, <sup>l</sup>D. Kirillov, <sup>a,c</sup>W. Klimala, <sup>f</sup>D. Kolev, <sup>n</sup>M. Kravčiková, <sup>o</sup>T. Kutsarova, <sup>j</sup>J. Lieb, <sup>a</sup>H. Machner, <sup>a,c</sup>A. Magiera, <sup>m</sup>G. Martinská, <sup>k</sup>H. Nann, <sup>e</sup>L. Pentchev, <sup>l</sup>N. Piskunov, <sup>a</sup>D. Protić, <sup>a</sup>P. von Rossen, <sup>b</sup>B. J. Roy, <sup>l</sup>I. Sitnik, <sup>d</sup>R. Siudak, <sup>a,m</sup>M. Uličný, <sup>c</sup>A. Strzałkowski, <sup>f</sup>R. Tsenov, <sup>a,g</sup>J. Urbán, <sup>b</sup>K. Zwoil

<sup>a</sup>Institut für Kernphysik, Forschungszentrum Jülich, Germany,

<sup>b</sup>Zentallabor für Elektronik, Forschungszentrum Jülich, Germany,

<sup>c</sup>Institute of Physics, Jagellonian University, Krakow, Poland,

<sup>d</sup>Institute of Nuclear Physics, Krakow, Poland,

<sup>e</sup>Institute of Nuclear Physics and Nuclear Energy, Sofia, Bulgaria,

<sup>f</sup>Physics Faculty, University of Sofia, Bulgaria,

<sup>g</sup>Institut für Strahlen – und Kernphysik der Universität Bonn, Germany,

<sup>h</sup>Institut für Kernphysik, Universität Münster, Germany,

<sup>i</sup>Nuclear physics Division, BARC, Bombay, India,

<sup>j</sup>Physics department, George Mason University, Fairfax, Virginia, USA,

<sup>k</sup>IUCF, Indiana University, Bloomington, Indiana, USA,

<sup>l</sup>LHE, JINR Dubna, Russia,

<sup>m</sup>P. J. Šafárik University, Košice, Slovakia,

<sup>n</sup>Technical University Košice, Slovakia.

## SUMMARY

A stack of annular detectors made of high purity germanium was used to measure  $p+d \rightarrow {}^3He+\pi^0$  and  $p+d \rightarrow {}^3H+\pi^\pm$  differential and total cross sections at beam momenta from 900 MeV/c to 1050 MeV/c. The total cross sections show to correspond to the  $\Delta$ -excitation. The differential data consist of two components. One corresponds to large momentum transfer from the projectile to the pion, the other to small momentum transfer. The former shows independence from the beam momentum in its form as function of the momentum transfer  $t$ . The slopes are different from  $\pi^+$  and  $\pi^0$  emission. The second component is almost isotropic and is approximately a quarter of the total yield in the  $\Delta$ -resonance region.

**Keywords:** cross sections, pion production, proton – deuteron collisions.

## 1. INTRODUCTION

The study of pion production in  $p+d$  collisions is expected to provide information about the underlying reaction dynamics. Various mechanisms involving participation of different number of nucleons as well as the response of the bound residual nuclei to high momentum transfers should be considered. The deuteron is a loosely bound system making it an ideal case for the use of impulse approximation. Also the knowledge of wave functions for  $A=2$  and  $A=3$  nuclei allows a more accurate treatment. At the experimental side, data for  $p+d \rightarrow {}^3He+\pi^0$  reaction exist near reaction threshold ( $\eta < 0.5$ ) where only the S-wave pion production is important and near the resonance region ( $\eta \approx 1.5$ ) where the  $\Delta$ -resonance is the dominant one. The data in the intermediate region, where S-D interference is expected to be large, are missing. The present experiments are performed to bridge the gap between these two intervals. The simultaneous detection of  $p+d \rightarrow {}^3H+\pi^\pm$  is also performed to investigate one of the most interesting aspects of strong interaction - the isospin invariance.

## 2. GEM DETECTORS AND TARGET SYSTEM

The experimental technique and methods are unique and differ from the ones used to study the above mentioned reactions. This new experimental design enabled a large angular acceptance (full solid angle) measurement with a very good energy resolution. The measurements were performed with the Germanium Wall of the GEM detector system. It is a stack of annular diodes made of high purity Ge. The first detector ( $\Delta E$ , quirl) is position sensitive segmented with 200 Archimedes spirals of opposite orientation on the front and rear sides. Each spiral from the front side crosses one spiral on the rear side defining thus 40000 pixels of sizes between 0.01-0.1 mm<sup>2</sup>. The quirl detector is 1.3 mm thick with a 5.8 mm diameter hole in the centre. It was followed by two E detectors (pizzas) segmented into 32 wedges. Each of these pizzas was 15 mm thick. The detector system accepts particles emitted between 50 and 290 mrad. In the present experiment a thinner 2.2 mm liquid deuterium target was used compared to the 6.4 mm applied in previous one. Details are given in [1].

### 3. RESULTS ON $p+d \rightarrow {}^3\text{He} + \pi^0$ AND $p+d \rightarrow {}^3\text{H} + \pi^\pm$ REACTIONS

The counts were lumped for each cms angular bin as a function of cms momenta or missing mass. Gaussian and smooth polynomial were fitted to the resulting spectra in order to separate the background. Finally the integrated counts in the Gaussians were converted to differential cross sections.

The cms angular distributions of  ${}^3\text{A}$  at lower energies are backward peaked - with an almost exponential slope. With increasing collision energy an isotropic component appears. This happens at large momentum transfers from the projectile to the ion, for illustration see Fig.1.

In order to study the two components of the angular distribution the relativistic invariant matrix element, directly connected also with  $d\sigma/dt$  was investigated -  $t$  being the four momentum transfer squared from proton to pion (see Fig.2 and Fig.3). The data are shown by dots, the fits by solid curves for the kinematically allowed range. The beam momenta in the laboratory system were in the region from 750 MeV/c to 1000 MeV/c. The data and fit curves are multiplied by the indicated factors.

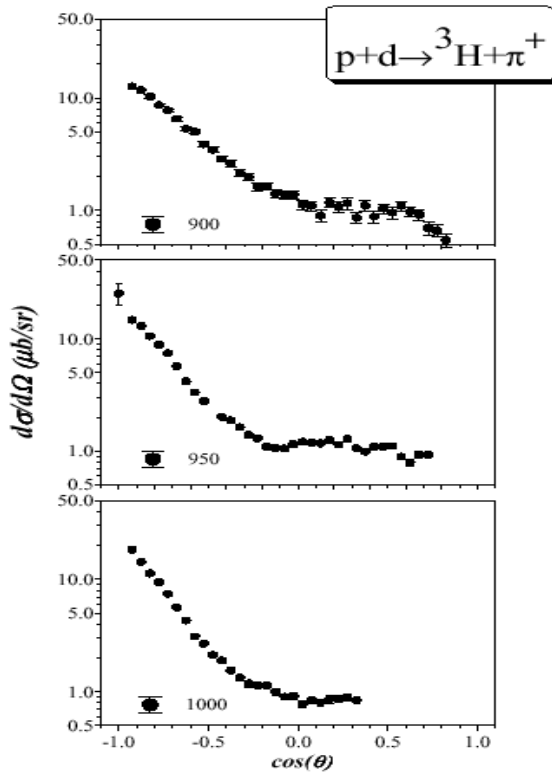


**Fig. 1** Differential cross sections for  $p+d \rightarrow {}^3\text{H} + \pi^\pm$  reaction as function of the cosines of  ${}^3\text{H}$  cms recoiling angle. The beam momenta are indicated in figure (MeV/c).

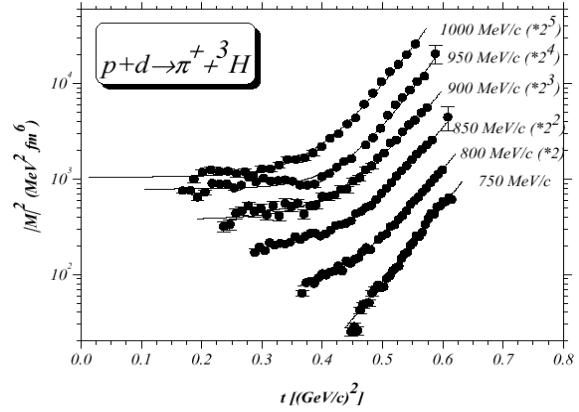


**Fig. 2** The  $t$ -dependence of the matrix elements squared for the  ${}^3\text{H} + \pi^\pm$  final channel.

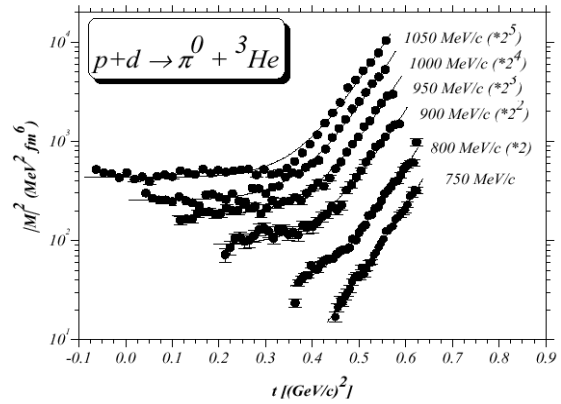


**Fig. 3** The same as Fig.2 but for  ${}^3\text{He} + \pi^0$  channel.

The behaviour of the matrix elements squared is the same as that of the angular distributions: an exponential component plus an almost  $t$ -independent part. However now the slopes of the steeply falling contributions are parallel. To be more specific we have fitted the function

$$|M(t)|^2 = a \exp(bt) + c$$

to the data. The results are rather uniform for  $b$ . They are:

$$b = 16.87 \pm 0.17 \text{ (GeV/c)}^{-2} \text{ for } \pi^0$$

$$b = 18.71 \pm 0.34 \text{ (GeV/c)}^{-2} \text{ for } \pi^\pm.$$

It is surprising that  $b$  is constant at 95% confidence level within 1% for  $\pi^0$  and 2% for  $\pi^\pm$  although the dimensionless variable  $\eta = p_\pi^*/m_\pi$  changes more than 1 unit for  $\pi^0$  (see Fig. 4).

In the Glauber approach applied to meson production on nuclei [2] the steep raising component is due to coherent, while the almost isotropic component is connected with incoherent meson production.

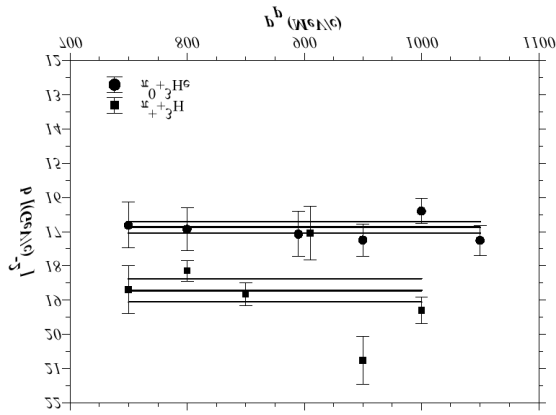


Fig. 4 The slope parameter  $b$  as obtained from fit to the data.

In the fitting procedure further parameter  $b$  is fixed and  $a$  and  $c$  are free. The results are shown in Figures 5 and 6 as functions of the dimensionless variable  $\eta$ . The values of  $a$  increase with increasing pion cms momenta and are slightly smaller for  $\pi^+$  than for  $\pi^0$  at a given beam energy.

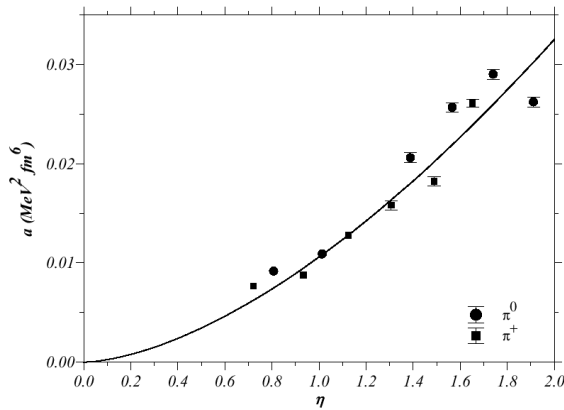


Fig. 5 The fit parameter  $a$  as a function of the pion centre mass momentum  $\eta = p^*_\pi / m_\pi$  with fixed values for  $b$ . The solid curve is to guide the eye.

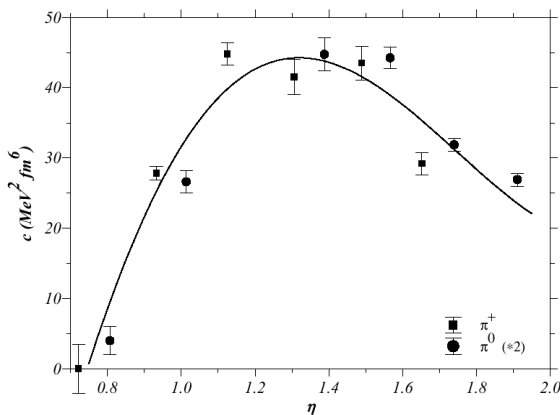


Fig. 6 The same as Fig. 5 but for the parameter  $c$ .

The fitted values for  $c$  seem to fulfill the isospin symmetry. On the figure the fit results for  ${}^3\text{He} + \pi^0$  final states are multiplied by isospin factor 2. Obviously the results obey this symmetry within the error bars. A smooth curve is fitted to the data to guide the eyes. The maximum at  $\eta \approx 1.3$  is below the  $\Delta$ -resonance.

The slope parameter  $b$  can be related to the strong absorption radius  $R$  of the optical potential model:

$$R = \sqrt[3]{b} hc$$

giving:

$$R = 1.622 \pm 0.008 \text{ fm for } {}^3\text{He} + \pi^0 \text{ and}$$

$$R = 1.708 \pm 0.016 \text{ fm for } {}^3\text{H} + \pi^+.$$

Similar analysis of the  $p+d \rightarrow p+d$  at 1 GeV/c yields  $b=15.4 \pm 1.3 \text{ (GeV/c)}^2$  [3] and an absorption radius  $R=1.55 \pm 0.07 \text{ fm}$ .

Most of the models applied to the present reactions are variations of the so called spectator model [4]. The  $t$ -dependence is due to a form factor, containing the deuteron and  $A=3$  wave functions and the more elementary  $N+N \rightarrow d+\pi$  cross section. One would naively expect  $R$  to scale down with the  ${}^3\text{He}$  and triton wave functions. However, the present results are in contrast with those for the charge radii from electron scattering:

$$r_{ch}({}^3\text{He}) = 1.959 \pm 0.030 \text{ fm} > r_{ch}({}^3\text{H}) = 1.755 \pm 0.086 \text{ fm}.$$

Since the Coulomb energy between the charged pion and triton is small the observed effect is probably due to Coulomb force between the two protons in the  ${}^3\text{He}$  wave function. In the entrance channel we are dealing with the same system, therefore another possibility for the different radii may be the different forces between the pions and  $A=3$  systems for the present partial waves involved.

Reaction cross sections were extracted fitting Legendre polynomials to the angular distributions. The found cross sections and the world data are shown as functions of  $\eta$ . In the case of  $p+d \rightarrow {}^3\text{He} + \pi^0$  reaction data are practically only in the threshold region as we can see in Fig. 7. The present data are shown as full dots, those from [5-9] by the indicated symbols. The dashed curve is the excitation function of the  $p+p \rightarrow d+\pi^+$  reaction scale down by a factor 72.2. The cross sections are also shown for the isotropic component. The solid curve is the cross section of  $p+p \rightarrow d+\pi^+$  scaled down by another factor 4.

For the reaction  $p+d \rightarrow {}^3\text{H} + \pi^+$  there were more data mainly from pion absorption, see Fig. 8. The dashed lines in figures display the properly scaled  $p+p \rightarrow d+\pi^+$  reaction. The wide peak around ( $d\pi^+$ )  $\eta \approx 1.6$  is due to  $\Delta$ -excitation. The  $A=3$  cross sections follow in the peak region the same dependence. The contribution of the isotropic part is similar as for  ${}^3\text{He} + \pi^0$  channel.

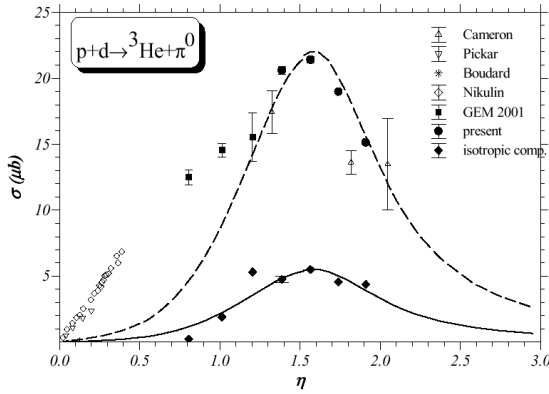


Fig. 7 Excitation function for the  $p+d \rightarrow {}^3\text{He}+\pi^0$  reaction as function of  $\eta = p^*_\pi/m_\pi$ .

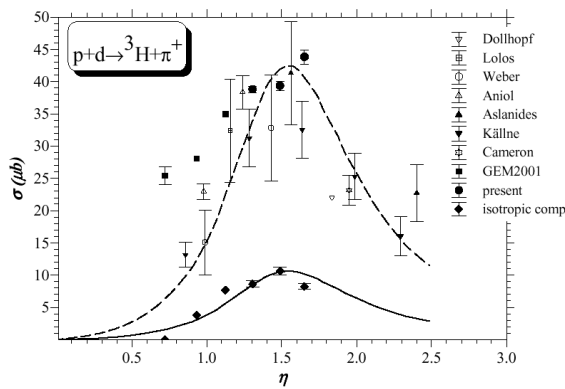


Fig. 8 The same as Fig. 7 but for  $p+d \rightarrow {}^3\text{H}+\pi^+$ .

The data points around the full curve in both (Figs.7 and 8) correspond to the extracted contribution of the isotropic part (parameter  $c$ ) which is approximately 25%. The momentum dependence again follow the  $\Delta$ -resonance excitation. The underlying reaction mechanism is presently unclear. It must be of a more complicated origin than the exponential part, since it is almost independent of the momentum transfer. Its onset at a certain collision energy and its coupling to the  $\Delta$  may shed light to this reaction mechanism.

#### 4. CONCLUSION

- ◆ Differential and total cross sections for the reactions  $p+d \rightarrow {}^3\text{He}+\pi^0$  and  $p+d \rightarrow {}^3\text{H}+\pi^+$  were measured in the  $\Delta$ -excitation region.
- ◆ The cms angular distributions show two components: one strongly increasing with momentum transfer to the pion and a smaller one almost independent on momentum transfer.
- ◆ Parametrization of  $d\sigma/dt = d\sigma/dt(t=0) \exp(bt) + d\sigma_0/dt$  yields constant values of slopes, but different for the two reactions.
- ◆ The slope parameters seem to carry more isospin information than  $d\sigma/dt(t=0)$ .

- ◆ The reaction mechanisms behind the  $d\sigma_0/dt \approx \text{const.}$  must be of more complicated nature than the exponential part, since it is independent of momentum transfer. Its onset corresponds to the threshold for  $N+N \rightarrow d+\pi$  reaction and needs further studies.

This work was in part supported by the Grant Agency for Science of the Ministry of Education, Slovak Republic (Grant No. 1/8041/01) and by German-Slovak bilateral project (No. Nem/Sl/BMBF2).

#### REFERENCES

- [1] Betigeri, M. et al.: Nucl. Instruments and Meth. in Phys. Res., **A 421**, 447 (1999)
- [2] Margolis, B., Kölbig, K. S.: Nucl. Phys., **B 86**, 85 (1968)
- [3] Booth, N. E. et al.: Phys. Rev., **D 4**, 1261(1971)
- [4] Ruderman, M.: Phys. Rev., **87**, 383 (1952)
- [5] Betigeri, M. et al.: Nucl. Phys., **A 690**, 473 (2001)
- [6] Boudard, A. et al.: Phys. Lett., **B 214**, 6 (1988)
- [7] Cameron, J. M. et al.: Nucl. Phys., **A 472**, 718 (1987)
- [8] Pickar, M. A. et al: Phys. Rev., **C 46**, 397 (1992)
- [9] Nikulin, V. et al.: Phys. Rev., **C 54**, 1732 (1996)